CrossMark

Forecasting of Multi-Step Ahead Reference Evapotranspiration Using Wavelet- Gaussian Process Regression Model

Masoud Karbasi[1]

Abstract Evapotranspiration is one of the most important components in the optimization of water use in agriculture and water resources management. In recent years, artificial intelligence methods and wavelet based hybrid model have been used for forecasting of hydrological parameters. In present study the application of the Gaussian Process Regression (GPR) and Wavelet-GPR models to forecast multi step ahead daily (1–30 days ahead) reference evapotranspiration at the synoptic station of Zanjan (Iran) were investigated. For this purpose a 10-year statistical period (2000–2009) was considered, 7 years (2000–2006) for training and the final three years (2007–2009) for testing the various models. Various combinations of input data (various lag times) and different kinds of mother wavelets were evaluated. Results showed that, compared to the GPR model, the hybrid model Wavelet-GPR had greater ability and accuracy in forecasting of daily evapotranspiration. Moreover, the use of yearly lag times in the GPR and wavelet-GPR model increased its accuracy. Investigation of various kinds of mother wavelets also indicated that the Meyer wavelet was the most suitable mother wavelet for forecasting of daily reference evapotranspiration. The results showed that by increasing the forecasting time period from 1 to 30 days, the accuracy of the models is reduced (RMSE = 0.068 mm/day for one day ahead and RMSE = 0.816 mm/day for 30 days ahead). Application of the proposed model to summer season showed that the performance of the model at summer season is better than its performance throughout the year.

Keywords Reference crop evapotranspiration · Forecasting · Time series · Wavelet · Gaussian Process regression

✉ Masoud Karbasi
  m.karbasi@znu.ac.ir

[1] Water Engineering Department, Faculty of Agriculture, University of Zanjan, Zanjan, Iran

🌊 Springer

1 Introduction

Water demand and consumption in agricultural ecosystems is heavily dependent on climatic parameters. In the planning and management of water resources for irrigation requirements, hydrological variables such as rainfall and evapotranspiration should be analyzed. Evapotranspiration (ET) is one of the key components of the hydrologic cycle and its accurate estimation is important for irrigation system design (Torres et al. 2011). Using past data of these variables and forecasting them is a key factor in planning, design and management of water resources. Application of long-term averaged of reference evapotranspiration value for upcoming days is a simple method, however because of climate change the results of this method may lead to large errors (Landeras et al. 2009). Given that the crop water requirements is calculated by multiplying reference evapotranspiration (ET_0) in the crop coefficient (K_c) (Allen et al. 1998), forecasting of reference crop evapotranspiration (ET_0) plays an important role in planning real time irrigation water requirements.

Time series models such as ARIMA and SARIMA have been used to forecast reference evapotranspiration in monthly and weekly time scales by various researchers (Landeras et al. 2009; Mariño et al. 1993; Meshram et al. 2015). However, using high resolution daily data is a limitation for the SARIMA model, since the season is 365 days which did not allow the model to converge (Bachour et al. 2016). Difficulties related to these models, motivated the researchers to use other modeling technics including data driven tools and statistical learning machines such as support vector machines (SVM), artificial neural networks (ANN), adaptive neuro-fuzzy interference system (ANFIS), Gaussian process regression (GPR) and decision trees. Trajkovic et al. (2003) used RBF neural networks to forecast monthly reference evapotranspiration. They used one and two year delay in their study. The results showed that RBF neural network is able to forecast monthly reference evapotranspiration with high accuracy. Landeras et al. (2009) used MLP (Multiple Layer Perceptron) and RBF (Radial Basis Function) neural networks to model future weekly reference evapotranspiration. In their research, two types of delays (weekly and yearly) were used. Their results showed that MLP and RBF neural networks can forecast weekly evapotranspiration with high confidence.

The GPR is a full Bayesian Non-parametric machine learning algorithm that has received significant attention in the machine learning community for applications such as model approximation, multivariate regression, and classification problems. Gaussian processes (GP) assume that the joint probability distribution of model outputs is Gaussian (Sun et al. 2014). Grbić et al. (2013) applied GRP model to predict water temperature of rivers. Their results showed that GPR model performs better than traditional approaches. Sun et al. (2014) used GRP to forecast monthly stream flow. Their results showed that GPR outperforms both linear regression and artificial neural network models. Hu and Wang (2015) used empirical wavelet transform-GRP model to forecast short-term wind speed. The new hybrid model can improve the forecasts in comparison of other models. Roushangar et al. (2016) used wavelet GRP hybrid model to forecast seepage through an earth dam. Applying different kernel functions, they concluded that RBF kernel function is superior to other kernel functions. Other applications of GRP model in modeling hydrological parameters have been reported (Grbić et al. 2013; Holman et al. 2014; Raghavendra and Deka 2016).

In recent years the use of hybrid models based on wavelet for forecasting hydrological time series (such as river flow, rainfall, ground water level and suspended sediment load) has attracted the attention of many researchers (Nourani et al. 2014). Gocić et al. (2015) used four soft computing technics: artificial neural network (ANN), support vector machine- firefly algorithm (SVM-FFA), genetic programming (GP) and support vector machine-Wavelet

(SVM-Wavelet) to forecast monthly ET0 at some meteorological stations of Serbia. Their results showed that SVM-Wavelet model has the highest accuracy for monthly ET0 forecasting. Bachour et al. (2016) used a hybrid model, Wavelet- multivariate relevance vector machine (MVRVM) to predict 16 days of future daily ET0. The results of the hybrid model showed that forecast of ET0 up to 16 days ahead reliably is possible ($R^2 = 0.619$ and RMSE = 0.766 mm/day for best model). Also their results showed that inclusion of 10-days of forecasted minimum and maximum air temperature as additional inputs can improve the performance of the model for 10 days forecast ($R^2 = 0.706$ and RMSE = 0.713 mm/day for best model). Also application of wavelet regression models has been reported in evapotranspiration estimation (Falamarzi et al. 2014; Kişi 2011; Partal 2009). Kişi (2011) showed that combination of discrete wavelet transform (DWT) and linear regression performs better than empirical equations in daily evapotranspiration modeling. Partal (2009) and Falamarzi et al. (2014) used discrete wavelet transform and artificial neural network (ANN) to model ET_0. Both of the results showed that combination of DWT and ANN performs better than single ANN model.

The first objective of present study is to forecast daily evapotranspiration at a semi-arid climate condition using a new hybrid wavelet-Gaussian process regression model. The second objective of this study is to forecast multistep ahead daily reference evapotranspiration and determination of best input data and model type to achieve higher accuracy in medium range evapotranspiration forecasts. The third Objective is to evaluate forecasts in different seasons of the year. Reviewing the previous researches shows that less attention has been paid in the forecasting of the reference evapotranspiration time series in more than one day ahead, and also in this research, the Gaussian process regression model is also used for the first time in the forecasting of reference evapotranspiration.

2 Materials and Methods

### 2.1 Study Area and Meteorological Data

In the present study, daily climatic data of minimum and maximum temperature, wind speed, sunshine hours and minimum and maximum relative humidity of Zanjan synoptic station (Fig. 1) (Longitude, 48°29′ E; Latitude, 36°41′ N; Elevation, 1663 m) was used to calculate the reference crop evapotranspiration. Meteorological data of the Zanjan synoptic station was available from 1980 to 2009, but the implementation of the model was difficult due to the use of daily weather data and the increase in the number of input data when using wavelet transforms. Therefore period of 2000 to 2009 was selected. The average temperature, annual rainfall and average daily evapotranspiration of Zanjan synoptic station are 11.1 °C, 311 mm and 2.8 mm per day respectively.

2.2 Penman-Monteith FAO-56 Model

In order to estimate daily reference evapotranspiration and create evapotranspiration time series, Penman-Monteith FAO-56 model was used (Allen et al. 1998):

$$\mathrm{ET}_0 = \frac{0.408\Delta(R_n - G)}{\Delta + \gamma(1 + 0.34u)} + \frac{900\gamma}{[\Delta + \gamma(1 + 0.34u)]} \frac{u(e_s - e_a)}{(T + 273)} \tag{1}$$

Where ET_0 is reference evapotranspiration (mm/day), T is mean daily air temperature at 2 m of ground surface (Celsius degrees), R_n is the net radiation at the surface vegetation (MJ /m²/
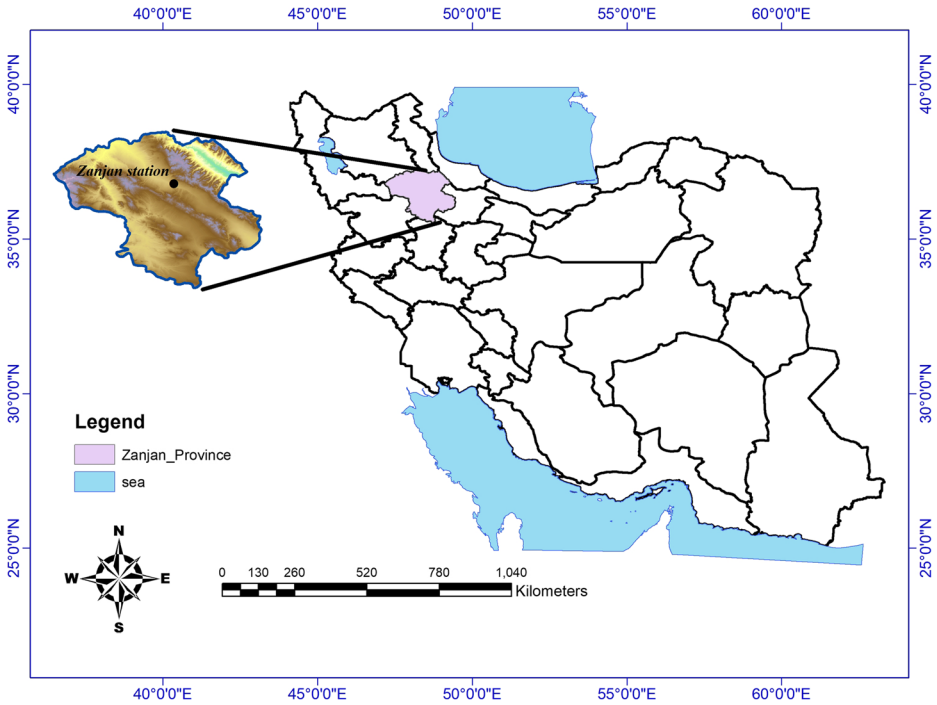
Fig. 1 Location of studying area

day), u is wind speed at height 2 m above the ground (m/s), $e_s - e_a$ is saturation vapor pressure deficit (kPa), γ is Psychrometric constant (kPa/°C), Δ slope of vapor pressure curve (kPa/°C), G ground heat flux (MJ /m²/day) (Allen et al. 1998). Equation 1 assumes that the plant height of 0.12 m and the reference grass surface resistance of 70 s per meter (Allen et al. 1998). At the above equation values of ground heat flux (G) for daily period are relatively low and can be neglected (Allen et al. 1998).

2.2.1 Our Available Data

In this study, a 10-year period 2000 to 2009 was selected. The first 7 years (2000–2006) were used as train data and remaining data (2007–2009) was considered as test data. Table 1 shows the statistical parameters of train and test dataset.

Table 1 Statistical parameters of train and test data

Variable	Data range		Mean		Standard deviation	
	Train	Test	Train	Test	Train	Test
T_{mean} (C°)	−16.4–28.7	−16.4–29.2	11.62	11.32	9.15	9.46
Wind speed (m/s)	0–11.98	0.25–13.27	2.96	2.71	1.17	1.23
Sunshine Hours (h)	0–13.8	0–13.6	8.09	7.64	3.92	3.62
Rain (mm)	0–44.6	0–39.4	0.79	0.779	2.76	2.82
ET_0 (mm/day)	0.32–9.54	0.17–8.85	3.69	3.45	2.27	2.09

2.3 Gaussian Process Regression

A Gaussian process (GP) is a probabilistic nonparametric model, where observations occur in a continuous domain (Grbić et al. 2013). It can be used for solving non-linear regression (Williams 1997) and classification (Williams and Barber 1998) problems. A Gaussian process regression directly defines a prior probability distribution over a latent function. GPR is specified by it mean function and covariance (kernel) function.

$$f(\mathbf{x}) \sim \mathrm{GP}\left(m(\mathbf{x}), k\left(\mathbf{x}, \mathbf{x}'\right)\right) \tag{2}$$

The mean function is often assumed zero, as it encodes central tendency of the function (Zhang et al. 2016). The covariance function encodes information about shape and structure of the function that we expect to have. The connection among input and output variables is expressed as

$$y = f(\mathbf{x}) + \varepsilon \tag{3}$$

It is assumed that noise ε is independent and a Gaussian distribution with zero mean and σ_n^2 variance is distributed over it.

$$\varepsilon \sim \mathcal{N}\left(0, \sigma_n^2\right) \tag{4}$$

According to Eq. (2), the likelihood is given by

$$p(\mathbf{y}|\mathbf{f}) = \mathcal{N}\left(\mathbf{y}|\mathbf{f}, \sigma_n^2 I\right) \tag{5}$$

Where $\mathbf{y} = [y_1, y_2, \ldots, y_n]^T$, $\mathbf{f} = [f(\mathbf{x}_1), f(\mathbf{x}_2), \ldots, f(\mathbf{x}_3)]$ and I is a $M \times M$ unit matrix.

According to definition of Gaussian process (MacKay 1998) the marginal distribution $p(\mathbf{f})$ is given by a Gaussian whose mean is zero and whose covariance is defined by a Gram matrix, so that

$$p(\mathbf{f}) = \mathcal{N}(\mathbf{f}|\mathbf{0}, K) \tag{6}$$

Where $K = k(x_i, x_j)$. Since both Eqs. (4) and (5) follow the Gaussian distribution, the marginal distribution of y is given by

$$p(\mathbf{y}) = \int p(\mathbf{y}|\mathbf{f}) p(\mathbf{f}) d\mathbf{f} = \mathcal{N}\left(\mathbf{f}|\mathbf{0}, K_y\right) \tag{7}$$

Where $K_y = K + \sigma_n^2 I$.

To predict the target variable y_* for a new input ($\mathbf{x}_*$), the joint distribution over $y_1, y_2, \ldots, y_m, y_*$ is given by

$$\begin{bmatrix} \mathbf{y} \\ y_* \end{bmatrix} = \left(\begin{bmatrix} \mathbf{f} \\ f_* \end{bmatrix} + \begin{bmatrix} \varepsilon \\ \varepsilon_* \end{bmatrix}\right) \sim \mathcal{N}\left(0, \begin{bmatrix} K_y & \mathbf{k}_* \\ \mathbf{k}_*^T & k_{**} + \sigma_n^2 \end{bmatrix}\right) \tag{8}$$

Where $f_* = f(\mathbf{x}_*)$ is the latent function for input variable $\mathbf{x}_*$ and ε_* is corresponding noise; $\mathbf{k}_* = [k(\mathbf{x}_*, \mathbf{x}_1), \ldots, k(\mathbf{x}_*, \mathbf{x}_M)]^T$ and $k_{**} = k(\mathbf{x}_*, \mathbf{x}_*)$. Application of the rules for conditioning

Gaussians (Bishop 2006), the predictive distribution $p(y_*|y)$ is a Gaussian distribution with mean and covariance given by

$$m(x_*) = \boldsymbol{k}_*^T K_y^{-1} \boldsymbol{y} \tag{9}$$

$$\sigma^2(\boldsymbol{x}_*) = k_{**} - \boldsymbol{k}_*^T K_y^{-1} \boldsymbol{k}_* + \sigma_n^2 \tag{10}$$

The Cholesky decomposition (Rasmussen and Williams 2006) can be used to calculate the inverse of the covariance matrix K_y. Equations (8) and (9) form the main results of GPR. The mean predictive distribution is used as point prediction and variance is used to evaluate the uncertainty of the prediction. The prediction interval calculation can be done using the predictive mean and variance. The 95% prediction interval is computed as $m(\mathbf{x}_*) \pm 1.96\sigma(\mathbf{x}_*)$ (according to the property of Gaussian distribution) (Zhang et al. 2016).

The covariance (kernel) function is acritical component in a Gaussian process regression. It encodes assumption about the function which wish to learn. In supervised learning similarity among data is very important. The covariance function defines this similarity (Rasmussen and Williams 2006). In this research, Squared Exponential covariance function was used

$$k\left(x_i, x_j | \theta\right) = \sigma_f^2 exp\left[-\frac{1}{2}\frac{\left(x_i - x_j\right)^T \left(x_i - x_j\right)}{\sigma_l^2}\right] \tag{11}$$

Where σ_l is the characteristic length scale and σ_f is the signal standard deviation. Hyper parameters of the covariance function θ (σ_l, σ_f) can be estimated from above equations by using a gradient-based algorithm (Rasmussen and Williams 2006).

2.4 Wavelet Decomposition

The wavelet transform of a continues time series $x(t)$, is defined as (Mallat 1989):

$$T(a,b) = \frac{1}{\sqrt{a}}\int_{-\infty}^{+\infty} g^*\left(\frac{t-b}{a}\right)x(t).dt \tag{12}$$

Where a is a scale factor, b is temporal translation of the $g(t)$, * corresponds to the complex conjugate and $g(t)$ is mother wavelet. Continues wavelet transform (CWT) decomposes the signal with large number of scale and translation parameters. Therefore, calculation of wavelet coefficients for all scales lead to large size of information. For practical applications, the hydrological time series are not continues signals but rather discrete time signals (Nourani et al. 2014). To overcome this, a logarithmically uniform spacing can be used for the a scale discretization with a correspondingly coarser resolution of the b locations, which allows for N transform coefficients to completely describe a signal of length N. Such a discrete wavelet has the form

$$g_{m,n}(t) = \frac{1}{\sqrt{a_0^m}}g\left(\frac{t-n\,b_0 a_0^m}{a_0^m}\right) \tag{13}$$

The most common values for a_0 and b_0 are 2 and 1 time steps, respectively. m and n are integers that control the wavelet dilation and translation. Mallat (1999) used

filters to develop an efficient way to implement this scheme. The DWT decompose the signal in to approximation (a) and details (d) components by passing the signal through the low-pass and high pass filters. The approximations and details components are high scale low frequency and low scale high frequency respectively. The most significant component of the signal is low frequency part, on the other hand, the high frequency component imparts nuance. For more details on the Wavelet transform readers are referred to text books including Daubechies (1992) and Wallen (2004).

2.5 Hybrid Model Structure

Main goal of wavelet-Gaussian process regression model is forecasting of daily reference evapotranspiration at a semi-arid region. To do this, firstly reference evapotranspiration time series were decomposed to approximation sub-series (A) (low frequency) and detail sub-series (D) (high frequency). In the next step, approximation and detail sub-series (A_1, D_1, D_2…, D_n) (where n is level of decomposition) were used as input matrix for wavelet-GPR model. Determination of mother wavelet type and level of decomposition plays an important role in model performance. In this research, debauches, symlet, coiflet and Meyer mother wavelets were used. Application of higher decomposition level can cause slower training process and in some cases can reduce the accuracy of the models. The following equation was used to select discrete wavelet transform decomposition level (Nourani et al. 2014).

$$L = Int[log(N)] \tag{14}$$

Where L is decomposition level, N is number of time series data and Int is floor function. In this study, all the proposed models are implemented using MATLAB 2016a software.

2.6 Model Input Data

In order to obtain the right combination of inputs to the model, several different combinations of input data was examined. Table 2 shows 10 different combinations of input data for 1 to 30 days ahead forecasting. The ET parameters used at Table 2, were calculated using Eq. (1).

Table 2 Different sets of model input and output variables for 1 to 30 days ahead forecasting

Output parameters	Input parameters	Model
ET_t-ET_{t+30}	ET_{t-1}	M1
ET_t-ET_{t+30}	ET_{t-1}, ET_{t-2}	M2
ET_t-ET_{t+30}	ET_{t-1}, ET_{t-2}, ET_{t-3}	M3
ET_t-ET_{t+30}	ET_{t-1}, ET_{t-2}, ET_{t-3}, ET_{t-4}	M4
ET_t-ET_{t+30}	ET_{t-1}, ET_{t-2}, ET_{t-3}, ET_{t-4}, ET_{t-5}	M5
ET_t-ET_{t+30}	ET_{t-1}, ET_{t-2}, ET_{t-3}, ET_{t-4}, ET_{t-5}, ET_{t-6}	M6
ET_t-ET_{t+30}	ET_{t-1}, ET_{t-2}, ET_{t-3}, ET_{t-4}, ET_{t-5}, ET_{t-6}, ET_{t-7}	M7
ET_t-ET_{t+30}	ET_{t-1}, ET_{t-2}, ET_{t-3}, ET_{t-4}, ET_{t-5}, ET_{t-365}	M8
ET_t-ET_{t+30}	ET_{t-1}, ET_{t-2}, ET_{t-3}, ET_{t-4}, ET_{t-5}, ET_{t-365}, ET_{t-730}	M9
ET_t-ET_{t+30}	ET_{t-1}, ET_{t-2}, ET_{t-3}, ET_{t-4}, ET_{t-5}, ET_{t-365}, ET_{t-730}, ET_{t-1095}	M10

2.7 Performance Evaluation Criteria

To evaluate the accuracy of the proposed models, following statistical measures were used:

$$RMSE = \sqrt{\frac{\sum_{i=1}^{N}(O_i - P_i)^2}{N}} \tag{15}$$

$$MBE = \frac{1}{N}\sum_{i=1}^{N}(O_i - P_i) \tag{16}$$

$$NRMSE = \frac{RMSE}{\overline{O_i}} \tag{17}$$

$$MAPE = \frac{1}{N}\sum_{i=1}^{N}\left|\frac{O_i - P_i}{O_i}\right| \times 100 \tag{18}$$

$$R^2 = \frac{\left(\sum_{i=1}^{N}(O_i - \bar{O}_i)\left(P_i - \bar{P}_i\right)\right)^2}{\sum_{i=1}^{N}(O_i - \bar{O}_i)^2 \sum_{i=1}^{N}(P_i - \bar{P}_i)^2} \tag{19}$$

At the above equations O_i and P_i respectively are observed and predicted values, $\bar{O}_i$ is the mean value of observations, $\bar{P}_i$ is the mean value of predictions and N is the total number of data. RMSE (Root Mean Square Error) is the measure of the differences between predicted and observed values. MAPE (Mean Absolute Percentage Error) is measure of prediction accuracy of the model. MBE (Mean Bias Error) is defined as the difference between the predicted values and true observed values. It is measure of over/under estimate of the model. The coefficient of determination R^2 describes the degree of association between the forecasted and the observed values. NRMSE (Normalized Root Mean Square Error) can be used to compare models with different scales. The performance of the model according to NRMSE is defined as follow (Mihoub et al. 2016):

Excellent if: NRMSE <10%
Good if: 10% < NRMSE <20%
Fair if: 20% < NRMSE <30%
Poor if: NRMSE >30%

3 Results

3.1 Gaussian Process Regression Model

Firstly simple GPR models are developed to forecast daily evapotranspiration. Data of daily evapotranspiration is used as model inputs. For wavelet-GPR hybrid models, the input evapotranspiration data is transformed using DWT. The transformed

evapotranspiration data is used as input in the development of wavelet-GPR models. Table 3 shows the results of single GPR model. For all of the time steps (days ahead) M1–M10 input models were implemented and the best model presented at Table 3.

According to Table 3 in the one-day ahead reference evapotranspiration forecast, the M4 model yielded the best result with RMSE = 0.678 mm / day and R2 = 0.896. Given that NRMSE = 19.6% is obtained, the model is evaluated as a good model. In forecasting of 2 to 30 days, the RMSE value increases and R^2 decreases with the increase of the forecasting time interval. In most models, the M10 input model provides the best result, indicating that the use of 365, 730, and 1095 daily delays can increase the accuracy of the model, while the one-day forecasting model annual delays could not increase accuracy of the model. In forecasting of 2 to 30 days, the value of the NRMSE parameter is between 21.1 and 25.5%, and the models are evaluated as fair models. Figure 2 shows the predicted evapotranspiration values against the results obtained from the PMF-56 equation for different forecasting periods.

Figure 3 demonstrates the point and interval predictions of reference evapotranspiration based on the single GPR model. It is obvious that nearly all the PMF-56 evapotranspiration data are within the 95% confidence interval.
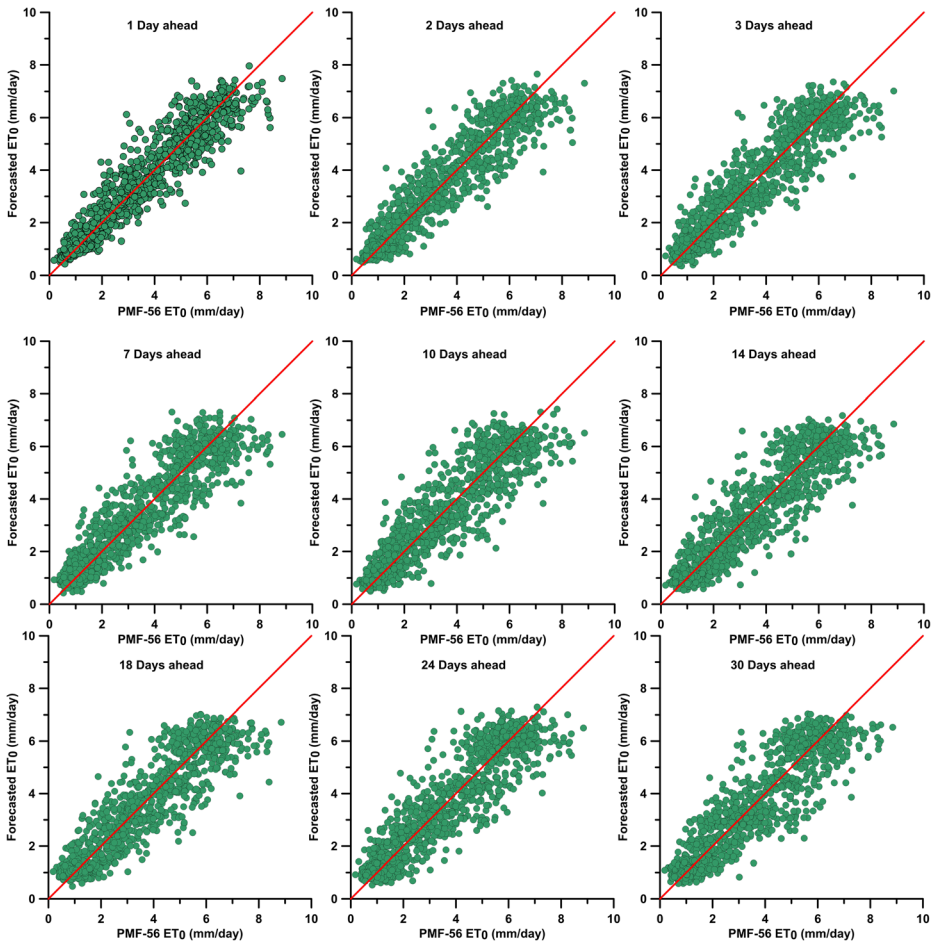
3.2 Wavelet-GPR Model

3.2.1 Effect of Wavelet Type

Proper selection of wavelet type (function) to decompose time series signal to approximation and details components is very important in the development of wavelet based hybrid models (Shoaib et al. 2015). To investigate effect of wavelet type on accuracy of the models, 10 mother wavelets (db1, db4, db8, sym2, sym4, sym8, coif1, coif3, coif5 and dmey) were selected. Results of application of different types of wavelet types on forecasting of one day ahead evapotranspiration has been shown at Table 4. According to Table 4, dmey (Meyer) type wavelet has the highest accuracy (RMSE = 0.068 mm/day). Coif5 (Coiflet) type mother wavelet is the second best Model (RMSE = 0.113 mm/day). Higher performance of Meyer type wavelet in modeling hydrological time series has been reported by Shoaib et al. (2015), Ebrahimi and

Table 3 Results of single GPR model for multi-step ahead evapotranspiration forecasting

Days ahead	Best Model	RMSE	R^2	MAPE(%)	MBE	NRMSE(%)
1	M4	0.678	0.896	18.7	−0.021	19.6
2	M10	0.765	0.868	22	0.008	22.1
3	M10	0.795	0.857	23.5	0.001	23
4	M8	0.817	0.849	24	−0.026	23.6
5	M10	0.829	0.844	24.2	0.004	24
7	M10	0.840	0.840	24.4	0.017	24.3
10	M9	0.864	0.831	24.2	0.024	25
12	M10	0.882	0.825	25.8	0.040	25.5
14	M10	0.871	0.830	25.9	0.061	25.2
16	M10	0.865	0.832	25.5	0.073	25
18	M10	0.853	0.837	24.8	0.075	24.6
21	M10	0.867	0.831	25.9	0.051	25.1
24	M10	0.870	0.829	26.4	0.033	25.1
27	M10	0.874	0.828	25.7	0.032	25.3
30	M10	0.861	0.833	24.9	0.037	24.9

Fig. 2 Forecasted evapotranspiration for 1–30 days ahead with single GPR model

Rajaee (2017) and Karbasi (2015). Because of higher performance of Meyer type wavelet, this type of wavelet were used for multi-step ahead (2–30 days) forecasting. Figure 4 shows the decomposed reference evapotranspiration time series using Meyer type wavelet (Table 4).

3.2.2 Multi Step Ahead Forecasting

Table 5 shows the results of the wavelet-GPR hybrid model in the forecasting of 1 to 30-days ahead reference evapotranspiration. According to Table 5, in the forecasting of a one-day ahead reference evapotranspiration, the M8 model provided the best result with RMSE = 0.068 mm day and R^2 = 0.999. The NRMSE value obtained for this model is 2%, and so the model is evaluated as an excellent model for forecasting evapotranspiration. By increasing the forecasting interval, the RMSE error value begins to increase. For example, the RMSE value has increased to 0.225 mm/day in the 2-days ahead forecasting of evapotranspiration. In the 7-days ahead forecast, the RMSE has increased to 0.458 mm per day. RMSE values in forecasting of 14, 21, and 30 days ahead evapotranspiration are 0.639, 0.818 and
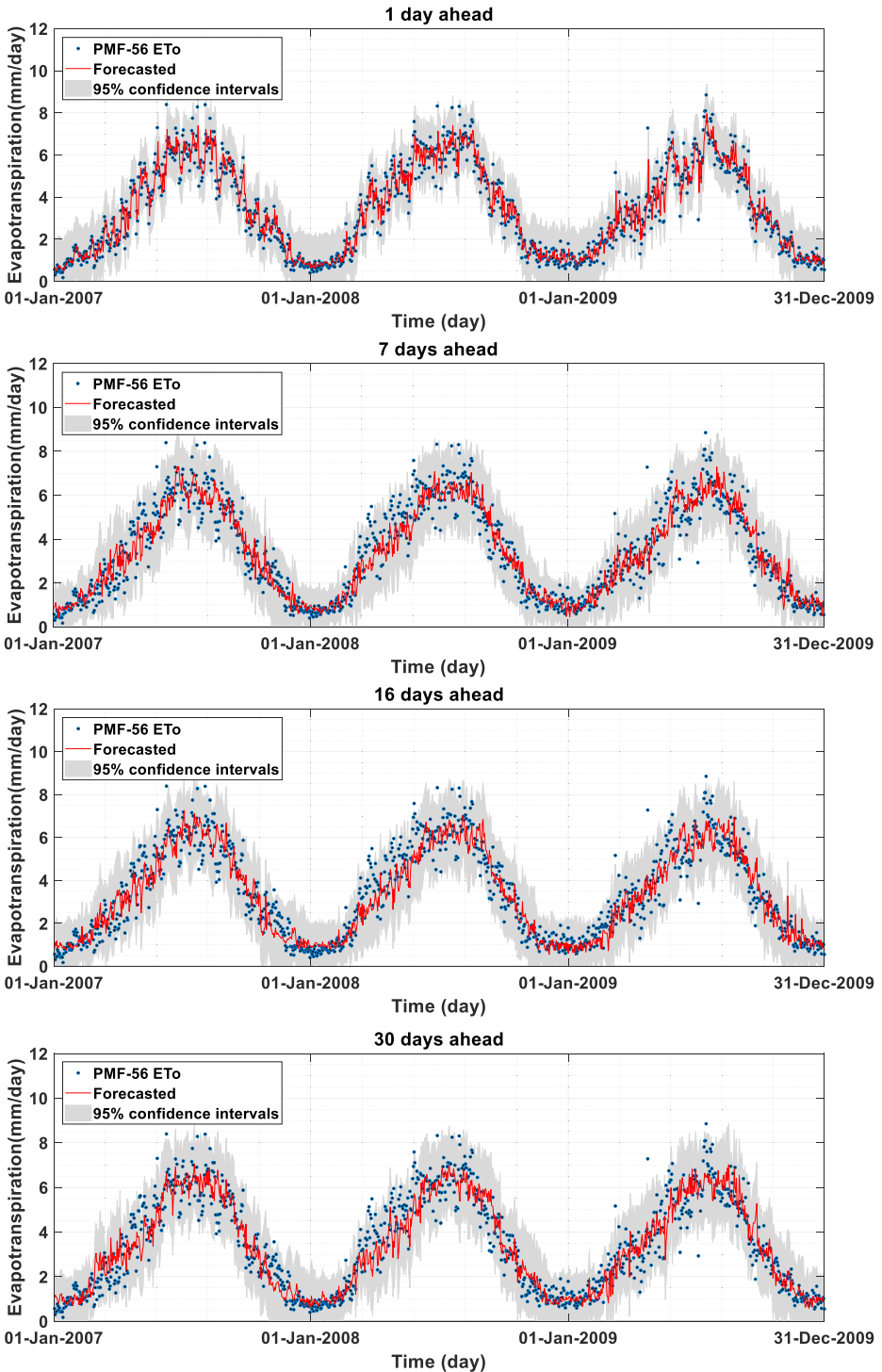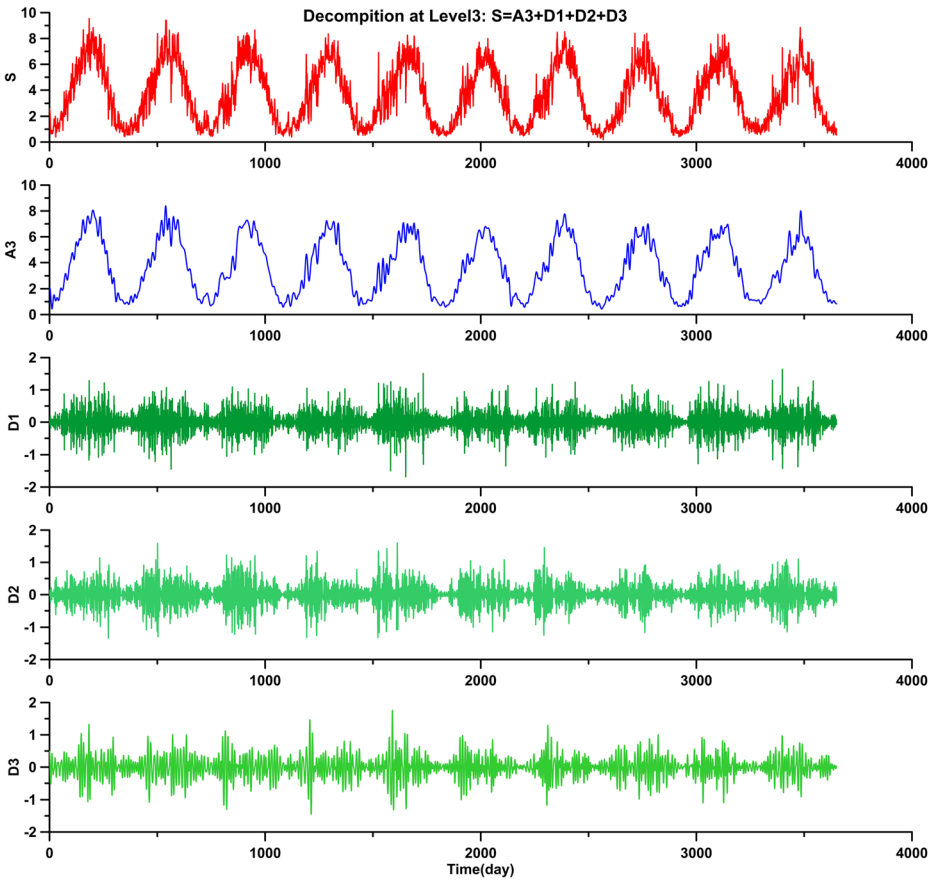
Fig. 3 point and interval forecasts of the evapotranspiration by single GPR model

**Fig. 4** Decomposed evapotranspiration time series using Meyer type wavelet

0.816 mm/day, respectively. The results of the wavelet-GPR model indicate that the proposed model is able to forecast 3-day ahead evapotranspiration with excellent precision (NRMSE value in the 3-day ahead forecast is 4.9%). In the forecasting of 4 to 14 days, the NRMSE value is between 10 and 20%, and the model is evaluated as a good model. In forecasting of 16 to 30 days, the NRMSE value is between 20 and 30%, and the models are evaluated as an average model. After a 16-days ahead forecast, the performance of the model is almost constant, with RMSE values higher than 0.8 mm per day. Examining the optimal combination of inputs to models shows that the M7, M8, M9 and M10 models have the best performance. The reason for this is the use of most of the above models in the history of the time series.

Table 4 Effect of the wavelet type on accuracy of forecasts

Model	M9	M7	M8	M10	M7	M7	M8	M7	M7	M7
wavelet type	db1	db4	db8	sym2	sym4	sym8	coif1	coif3	coif5	dmey
RMSE	0.415	0.213	0.138	0.315	0.207	0.132	0.308	0.15	0.113	0.068
R^2	0.961	0.99	0.996	0.977	0.99	0.996	0.979	0.995	0.997	0.999

Table 5 Results of Wavelet-GPR model for multi-step ahead evapotranspiration forecasting

Days ahead	Best Model	RMSE	R2	MAPE(%)	MBE	NRMSE(%)
1	M8	0.068	0.999	1.8	0.000	2
2	M8	0.225	0.988	6.1	0.000	6.5
3	M10	0.324	0.976	8.8	−0.001	9.4
4	M7	0.357	0.971	10.1	0.003	10.3
5	M7	0.400	0.964	11.3	0.001	11.6
7	M10	0.458	0.952	13.1	0.003	13.2
10	M8	0.519	0.939	14.8	−0.002	15
12	M10	0.582	0.923	17	0.025	16.8
14	M8	0.639	0.907	18.4	−0.010	18.5
16	M8	0.742	0.876	21.3	−0.005	21.4
18	M10	0.800	0.857	24.5	0.058	23.1
21	M10	0.818	0.850	24.9	0.045	23.6
24	M10	0.831	0.845	25.2	0.020	24
27	M9	0.823	0.848	25.1	0.016	23.8
30	M9	0.816	0.851	24.8	0.013	23.6
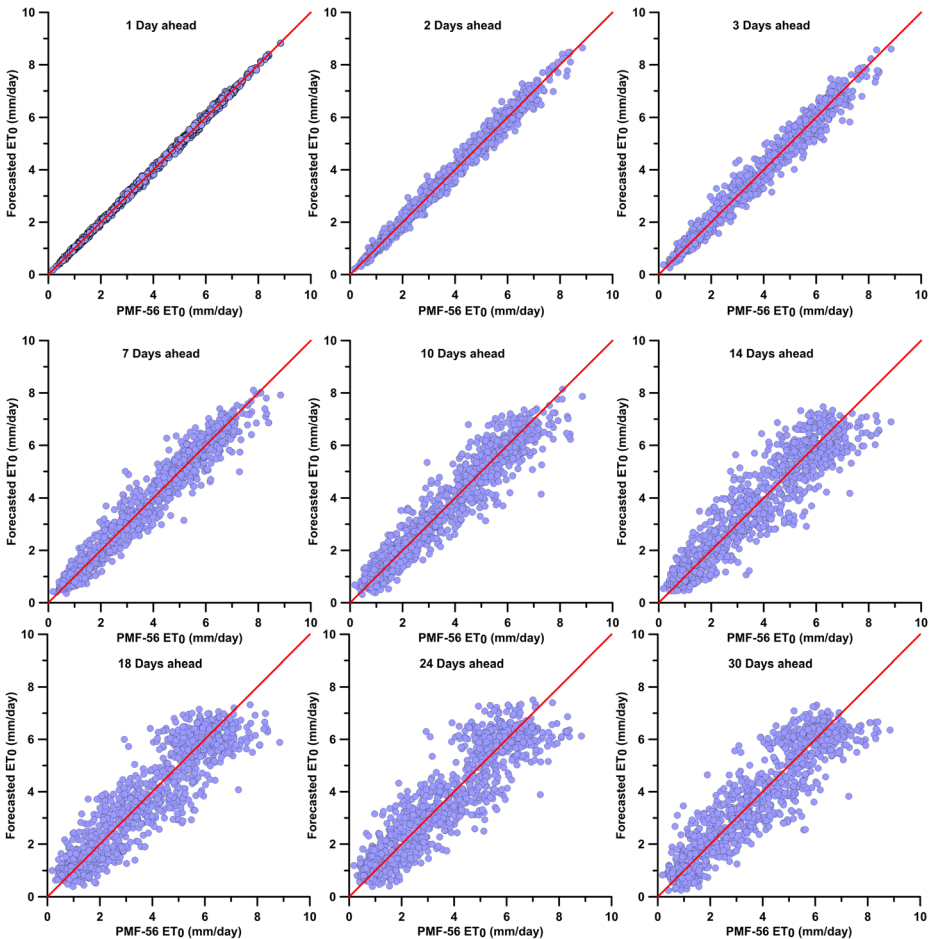
Fig. 5 Forecasted evapotranspiration for 1–30 days ahead with Wavelet- GPR model
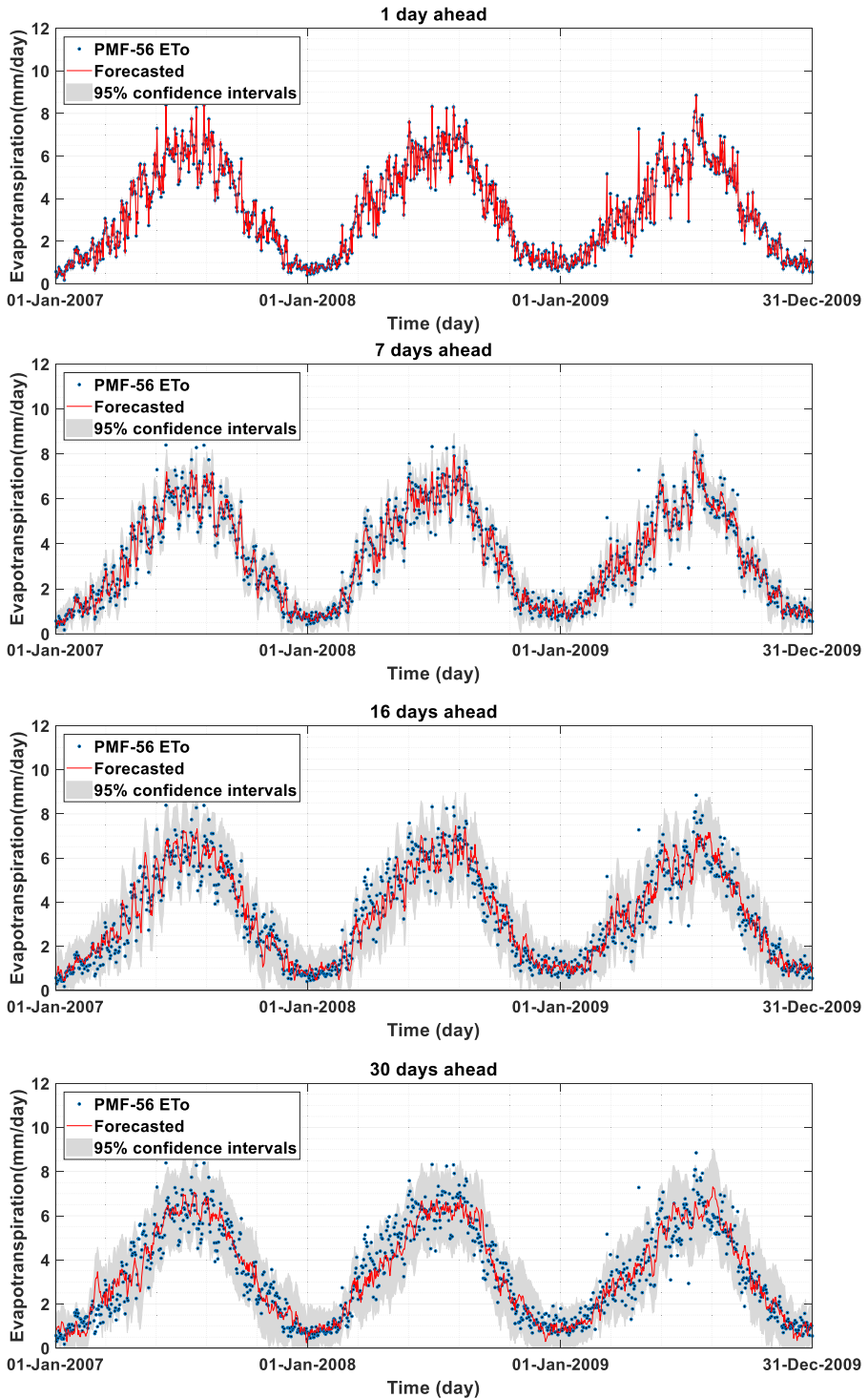
Fig. 6 point and interval forecasts of the evapotranspiration by Wavelet GPR model

Figure 5 shows the forecasted evapotranspiration values using wavelet-GPR model against the results obtained from the PMF-56 equation for different forecasting periods.

Figure 6 demonstrates the point and interval predictions of reference evapotranspiration based on the hybrid Wavelet-GPR model. It is obvious that nearly all the PMF-56 evapotranspiration data are within the 95% confidence interval.

According to Tables 3 and 5, comparison of GPR and wavelet-GPR models shows that the pre-processing of data using wavelet transform and utilizing it as GPR model input, greatly increases the accuracy of the model in forecasting daily Evapotranspiration. This result is reported by many researchers who compared wavelet-based hybrid models with non-wavelet models (Adamowski and Chan 2011; Nourani et al. 2014; Ramana et al. 2013). Bachour et al. (2016) using the MRVM method and combining it with wavelet transform, forecasted reference evapotranspiration for the next 16 days. Their results showed that the use of wavelet transformation as a preprocessor can increase forecasting performance of the model.

In the superiority of wavelet-based models, it can be stated that the complex hydrological time series is decomposed using a discrete wavelet transform into simple time series; therefore, some of the features of the time series, such as the daily, weekly, monthly and yearly periods, are clearly more visible. This excellence can be seen even in wavelet regression models. Kişi (2011), Partal (2016) and Patil and Deka (2017) analyzed the parameters related to reference evapotranspiration using a discrete wavelet transform and used them as inputs of different models. Their results also showed that the use of wavelet transformation in pre-processing of input data has increased the accuracy of the estimation of reference evapotranspiration.

3.3 Model Evaluation at Summer Season

The developed model in the previous section have been used to forecast reference evapotranspiration throughout the entire year, while the plant's growing season is in the spring and summer seasons. To evaluate the performance of the proposed model,

Table 6 Results of Wavelet-GPR model for multi-step ahead evapotranspiration forecasting at summer season

Days ahead	RMSE	R2	MAPE(%)	MBE	NRMSE(%)
1	0.085	0.996	1.3	0.001	1.5
2	0.281	0.952	4.2	0.002	5.0
3	0.385	0.909	5.9	−0.001	6.9
4	0.402	0.901	6.1	0.008	7.2
5	0.460	0.870	6.9	0.010	8.2
7	0.517	0.836	7.7	0.003	9.3
10	0.596	0.782	8.7	−0.026	10.7
12	0.658	0.734	9.8	−0.023	11.8
14	0.744	0.662	11.3	−0.053	13.3
16	0.871	0.539	13.6	−0.047	15.6
18	0.922	0.485	14.2	−0.050	16.5
21	0.948	0.461	14.9	−0.098	17.0
24	0.977	0.435	15.0	−0.094	17.5
27	0.966	0.436	15.4	−0.097	17.3
30	0.966	0.437	15.5	−0.093	17.3

the results of the model were evaluated in summer. The period from June 22 to September 22 of test data (2007–2009) was considered as summer. The mean value of reference evapotranspiration at summer is 5.59 mm/day. Table 6 shows the results of the wavelet-GPR model in the forecasting of the reference evapotranspiration in summer in the 1 to 30 days later. According to the results of Table 6, with the increase of the forecasted time interval, the RMSE value increased from 0.085 mm/day for one day forecast to 0.996 mm/day for 30 days forecast. Investigating the value of E also shows that, up to 7 days ahead, the performance of the model is evaluated as excellent model (NRMSE <10%). In forecasting of 10 to 30 days later, the NRMSE value is between 10 and 20, which is a good model. The results in this section show that model performance in the warm season is better than its performance throughout the year. Figure 7 shows the forecasted evapotranspiration values using wavelet-GPR model against the results obtained from the PMF-56 equation for different forecasting periods at summer season.
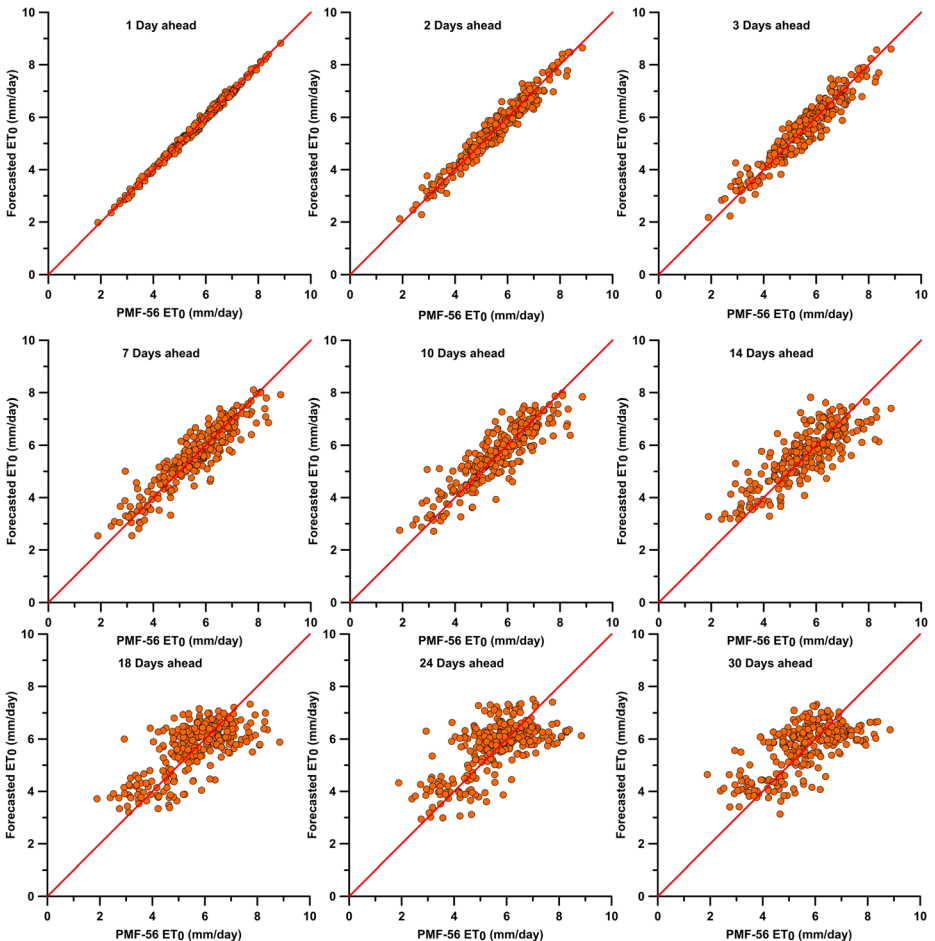

Fig. 7 Forecasted evapotranspiration for 1–30 days ahead with Wavelet- GPR model at summer season

4 Conclusion

The forecasting of reference evapotranspiration and crop water requirement of different plants can be helpful in the management of water resources. The results of this study showed that two wavelet-GPR and GPR models can forecast daily evapotranspiration with high accuracy. Although the GPR model is capable of modeling nonlinear behavior, but due to the non-stationary behavior of the daily evapotranspiration time series, for more accurate modeling, there is a need for the processing of input data into the model. Wavelet transformation by separating the signal into high frequencies and the low-frequency features of the signal increased the accuracy of the model. The comparison between the wavelet types showed that the Meyer type wavelet could increase the accuracy of the forecast due to its higher complexity and similarity to the daily reference evapotranspiration time series. According to the NRMSE criteria, the forecasting of 1–3 days ahead of reference evapotranspiration was classified as an excellent model (NRMSE <10). While in the forecasting of 4 to 14 days ahead (10 < NRMSE < 20) the model was classified as a good model and in the forecasting of 16 to 30 days ahead, the model was classified as an average model. This result shows that the model is not accurate in forecasting of 16 to 30 days ahead evapotranspiration, and it is suggested that in the future research, the meteorological forecasts should be used as the input of the model. The results of this research can be used for irrigation planning and optimal water use in studied areas. It is suggested that the proposed model be investigated in different climate conditions.

Compliance with Ethical Standards

Conflict of Interest The authors declare that they have no conflict of interest.

References

Adamowski J, Chan HF (2011) A wavelet neural network conjunction model for groundwater level forecasting. J Hydrol 407:28–40

Allen RG, Pereira LS, Raes D, Smith M (1998) Crop evapotranspiration-Guidelines for computing crop water requirements-FAO Irrigation and drainage paper 56 FAO. Rome 300:D05109

Bachour R, Maslova I, Ticlavilca AM, Walker WR, McKee M (2016) Wavelet-multivariate relevance vector machine hybrid model for forecasting daily evapotranspiration. Stoch Env Res Risk A 30:103–117. https://doi.org/10.1007/s00477-015-1039-z

Bishop CM (2006) Pattern recognition. Mach Learn 128:1–58

Daubechies I (1992) Ten lectures on wavelets. SIAM

Ebrahimi H, Rajaee T (2017) Simulation of groundwater level variations using wavelet combined with neural network, linear regression and support vector machine. Glob Planet Chang 148:181–191. https://doi.org/10.1016/j.gloplacha.2016.11.014

Falamarzi Y, Palizdan N, Huang YF, Lee TS (2014) Estimating evapotranspiration from temperature and wind speed data using artificial and wavelet neural networks (WNNs). Agric Water Manag 140:26–36. https://doi.org/10.1016/j.agwat.2014.03.014

Gocić M, Motamedi S, Shamshirband S, Petković D, Ch S, Hashim R, Arif M (2015) Soft computing approaches for forecasting reference evapotranspiration. Comput Electron Agric 113:164–173. https://doi.org/10.1016/j.compag.2015.02.010

Grbić R, Kurtagić D, Slišković D (2013) Stream water temperature prediction based on Gaussian process regression. Expert Syst Appl 40:7407–7414. https://doi.org/10.1016/j.eswa.2013.06.077

Holman D, Sridharan M, Gowda P, Porter D, Marek T, Howell T, Moorhead J (2014) Gaussian process models for reference ET estimation from alternative meteorological data sources. J Hydrol 517:28–35. https://doi.org/10.1016/j.jhydrol.2014.05.001

Hu J, Wang J (2015) Short-term wind speed prediction using empirical wavelet transform and Gaussian process regression. Energy 93(Part 2):1456–1466. https://doi.org/10.1016/j.energy.2015.10.041

Karbasi M (2015) Forecasting of Daily Reference Crop Evapotranspiration Using Wavelet- Artificial Neural Network Hybrid Model (In Persian) Iranian. J Irrig Drain 9:761–772

Kişi Ö (2011) Evapotranspiration modeling using a wavelet regression model. Irrig Sci 29:241–252. https://doi.org/10.1007/s00271-010-0232-6

Landeras G, Ortiz-Barredo A, López JJ (2009) Forecasting Weekly Evapotranspiration with ARIMA and Artificial Neural Network Models. J Irrig Drain Eng 135:323–334. https://doi.org/10.1061/(ASCE)IR.1943-4774.0000008

MacKay DJ (1998) Introduction to Gaussian processes NATO ASI Series F. Comp Syst Sci 168:133–166

Mallat SG (1989) A theory for multiresolution signal decomposition: the wavelet representation. IEEE Trans Pattern Anal Mach Intell 11:674–693

Mallat S (1999) A wavelet tour of signal processing. Academic press

Mariño MA, Tracy JC, Taghavi SA (1993) Forecasting of reference crop evapotranspiration. Agric Water Manag 24:163–187. https://doi.org/10.1016/0378-3774(93)90022-3

Meshram D, Gorantiwar S, Mittal H, Jain H (2015) Forecasting of Pomegranate (Punica granatum L.) evapotranspiration by using Seasonal ARIMA Model. Indian J Soil Conserv 43:38–46

Mihoub R, Chabour N, Guermoui M (2016) Modeling soil temperature based on Gaussian process regression in a semi-arid-climate, case study Ghardaia, Algeria. Geomech Geophys Geo-Energy Geo-Resourc 2:397–403. https://doi.org/10.1007/s40948-016-0033-3

Nourani V, Hosseini Baghanam A, Adamowski J, Kisi O (2014) Applications of hybrid wavelet–Artificial Intelligence models in hydrology: A review. J Hydrol 514:358–377. https://doi.org/10.1016/j.jhydrol.2014.03.057

Partal T (2009) Modelling evapotranspiration using discrete wavelet transform and neural networks. Hydrol Process 23:3545–3555. https://doi.org/10.1002/hyp.7448

Partal T (2016) Comparison of wavelet based hybrid models for daily evapotranspiration estimation using meteorological data KSCE. J Civ Eng 20:2050–2058

Patil AP, Deka PC (2017) Performance evaluation of hybrid Wavelet-ANN and Wavelet-ANFIS models for estimating evapotranspiration in arid regions of India. Neural Comput & Applic 28:275–285

Raghavendra NS, Deka PC (2016) Multistep Ahead Groundwater Level Time-Series Forecasting Using Gaussian Process Regression and ANFIS. In: Chaki R, Cortesi A, Saeed K, Chaki N (eds) Advanced Computing and Systems for Security: Volume 2. Springer India, New Delhi, pp 289–302. https://doi.org/10.1007/978-81-322-2653-6_19

Ramana RV, Krishna B, Kumar S, Pandey N (2013) Monthly rainfall prediction using wavelet neural network analysis. Water Resour Manag 27:3697–3711

Rasmussen CE, Williams CK (2006) Gaussian processes for machine learning. 2006 The MIT Press, Cambridge, MA, USA 38:715-719

Roushangar K, Garekhani S, Alizadeh F (2016) Forecasting Daily Seepage Discharge of an Earth Dam Using Wavelet–Mutual Information–Gaussian Process Regression Approaches. Geotech Geol Eng 34:1313–1326. https://doi.org/10.1007/s10706-016-0044-4

Shoaib M, Shamseldin AY, Melville BW, Khan MM (2015) Runoff forecasting using hybrid Wavelet Gene Expression Programming (WGEP) approach. J Hydrol 527:326–344. https://doi.org/10.1016/j.jhydrol.2015.04.072

Sun AY, Wang D, Xu X (2014) Monthly streamflow forecasting using Gaussian Process Regression. J Hydrol 511:72–81. https://doi.org/10.1016/j.jhydrol.2014.01.023

Torres AF, Walker WR, McKee M (2011) Forecasting daily potential evapotranspiration using machine learning and limited climatic data. Agric Water Manag 98:553–562. https://doi.org/10.1016/j.agwat.2010.10.012

Trajkovic S, Todorovic B, Stankovic M (2003) Forecasting of Reference Evapotranspiration by Artificial Neural Networks. J Irrig Drain Eng 129:454–457. https://doi.org/10.1061/(ASCE)0733-9437(2003)129:6(454)

Wallen RD (2004) The illustrated wavelet transform handbook. Biomed Instrum Technol 38:298–298

Williams CK (1997) Regression with Gaussian processes. In: Mathematics of Neural Networks. Springer, pp 378–382

Williams CKI, Barber D (1998) Bayesian classification with Gaussian processes. IEEE Trans Pattern Anal Mach Intell 20:1342–1351. https://doi.org/10.1109/34.735807

Zhang C, Wei H, Zhao X, Liu T, Zhang K (2016) A Gaussian process regression based hybrid approach for short-term wind speed prediction. Energy Convers Manag 126:1084–1092. https://doi.org/10.1016/j.enconman.2016.08.086